

# Ultrasonic Impact Treatment to Improve Stress Corrosion Cracking Resistance of Welded Joints of Aluminum Alloy

J. Yu, G. Gou, L. Zhang, W. Zhang, H. Chen, and Y.P. Yang

(Submitted May 28, 2015; in revised form January 31, 2016; published online June 8, 2016)

Stress corrosion cracking is one of the major issues for welded joints of 6005A-T6 aluminum alloy in high-speed trains. High residual stress in the welded joints under corrosion results in stress corrosion cracking. Ultrasonic impact treatment was used to control the residual stress of the welded joints of 6005A-T6 aluminum alloy. Experimental tests show that ultrasonic impact treatment can induce compressive longitudinal and transverse residual stress in the welded joint, harden the surface, and increase the tensile strength of welded joints. Salt-fog corrosion tests were conducted for both an as-welded sample and an ultrasonic impact-treated sample. The surface of the treated sample had far fewer corrosion pits than that of the untreated sample. The treated sample has higher strength and lower tensile residual stress than the untreated sample during corrosion. Therefore, ultrasonic impact treatment is an effective technique to improve the stress corrosion cracking resistance of the welded joints of 6005A-T6 aluminum alloy.

**Keywords** aluminum alloy, corrosion, high-speed trains, residual stress, ultrasonic impact treatment, welding

## 1. Introduction

Aluminum alloy 6005 A is a medium-strength, heat-treatable alloy with very good extrusion capability. It has been used in intricate extrusions in high-speed trains such as underframes, sidewalls, and front head. Although the body structure made of 6005A-T6 aluminum alloy is designed to meet the strength requirement, stress corrosion cracking (SCC) in the welded joints occurs during service because high-speed electric multiple unit (EMU) trains experience various corrosive environments. Some research results show that the corrosion occurs in the presence of hostile chemical species, such as chlorine ions, sulfide, nitrogen compounds, carbonate, and organics (Ref 1-6). High residual stress in the weld joints under corrosion induces SCC initiation and propagation, that results in the fracture of the high-speed train's body structures (Ref 7).

High-speed trains include numerous butt joints, lap joints, fillet joints, and cross joints in the body structures. Stress concentration and high residual stress exist in the welded joints (Ref 8) which affect the structure's capability to resist fatigue, brittle fracture, and SCC. Gou et al. (Ref 9) found that the maximum tensile stress was approximately 157.3 MPa, which was close to the yield strength of the base material A6N01S-T5

aluminum alloy and far beyond the design allowable stress 39 MPa (Ref 10). Therefore, controlling the weld residual stress is important to improve the failure resistance of welded joints that result from fatigue and SCC.

There are no standard methods in SCC improvement. SCC can be improved by either eliminating the corrosive environment or reducing weld tensile residual stress at the welded joints. Control of weld tensile residual stress has been the effective method to reduce the tendency of SCC since the corrosion environment cannot be changed in most applications. A wide variety of techniques (Ref 11, 12) are available for the reduction or modification of weld residual stress distributions. Some of these, such as post-weld heat treatment (PWHT) (Ref 13), vibration stress relief (VSR) (Ref 14), localized cooling (Ref 15), mechanical rolling (Ref 15), laser shock peening (Ref 16, 17), hammer and shot peening (Ref 18), and ultrasonic impact treatment (UIT) (Ref 19-28), have been adapted or optimized for mitigating weld residual stress. Recently, the micro-arc oxidation (MAO) process was applied to the surface treatment of an A7N01 alloy welded joint to improve the residual stress distribution and its properties. Oxide ceramic coating with a thickness of 13  $\mu\text{m}$  was prepared on the surface of the welded joints. The resulting residual stress of the welded joint decreased significantly. However, the coating process is very expensive, can only be used in small parts, and cannot be applied to all welded joints in EMU trains (Ref 29).

PWHT (Ref 13) can be conducted by heating the entire welded structure in a furnace or the welded joint locally to allow residual stress relaxation. For high-speed EMU trains, only local heating can be applied since the structure is too large to place in a furnace. Although PWHT is effective at reducing weld residual stress, it cannot be used to treat the welded joints of A6N01S-T5 aluminum alloy because the local heating will destroy the original material heat treatment conditions and result in a lower joint strength. VSR (Ref 14) was developed during the World War II. In this method, the welded object is simply vibrated using motorized or electromagnetic equipment. Despite many years of research, there is still disagreement over the fundamental mechanism and the effectiveness of this technique. Localized cooling (Ref 15) uses an intense heat sink

J. Yu, Traction Power State Key Laboratory, Southwest Jiaotong University, Chengdu 610031, China; and CNR Tangshan Co., Ltd., Tangshan 063035, China; G. Gou and H. Chen, School of Material Science and Engineering, Southwest Jiaotong University, Chengdu 610031, China; L. Zhang and W. Zhang, Traction Power State Key Laboratory, Southwest Jiaotong University, Chengdu 610031, China; and Y.P. Yang, Edison Welding Institute (EWI), Columbus, OH 43221. Contact e-mails: tpl@home.swjtu.edu.cn and yyang@ewi.org.

trailing the welding heat source to create a characteristic valley-shaped temperature distribution to reduce weld deformation and residual stress. This technique is good for long welds and difficult to apply to the complicated welded joints in high-speed EMU trains. Similarly, mechanical rolling (Ref 15) is difficult to implement in the welding of EMU trains.

Laser shock peening (Ref 16, 17), hammer and shot peening (Ref 18), and UIT (Ref 19) have a similar principal for controlling weld residual stress. All use impact or the propagation of shock waves to cause deformation on a welded joint to create an inherent strain which results in a compressive state of residual stress. While hammer and shot peening of welds have long been practiced, similar treatments such as needle, ultrasonic, and laser shock peening are becoming more widespread. Laser shock peening is more expensive and less flexible than hammer and shot peening and UIT since it

involves laser equipment. UIT is easy to operate and more efficient than hammer and shot peening. Therefore, UIT was selected to improve the SCC of welded joints of A6N01S-T5 aluminum alloy in this study.

UIT has been confirmed to be one of the best preventative treatment methods to reduce tensile residual stresses or produce favorable compressive residual stress and locally modify the weld geometry to improve fatigue performance and prolong fatigue life (Ref 19-28). UIT can also refine the microstructure grain size of 2024-T351 aluminum alloy (Ref 24) and stainless steel 304 (Ref 25) to improve the material properties. Recently, UIT was used to improve corrosion resistance of welded joints of 304 stainless steel (Ref 26), 16MnR steel (Ref 27), and ferritic-martensitic steels (Ref 28). The microstructure observation results revealed that a hardened layer was formed on the surface, and the initial coarse-grained structure in the surface

**Table 1 Chemical compositions of base materials and filler metal**

Materials	Chemical composition, wt.%									
	Zn	Mg	Cu	Mn	Cr	Ti	Zr	Si	Fe	Al
6005A	≤ 0.20	0.4-0.7	≤ 0.30	≤ 0.50	≤ 0.30	≤ 0.10	0.000	≤ 0.40	≤ 0.40	Bal.
ER5356	≤ 0.10	4.5-5.5	≤ 0.10	0.05-0.20	0.05-0.20	0.06-0.2	0.000	≤ 0.25	≤ 0.10	Bal.

**Table 2 Mechanical properties of base materials and filler metal**

Materials	Hardness, HV	Tensile strength, MPa	Yield strength, MPa	Elongation, %	Fatigue strength, MPa
A6005-T6	100	260	240	8	100
ER5356	...	207	131	11	...

**Table 3 Welding process parameters**

Materials	Thickness, mm	Pass	Current, A	Voltage, V	Welding speed, mm/s
6005A-T6	4	1	230-280	24-30	6.7

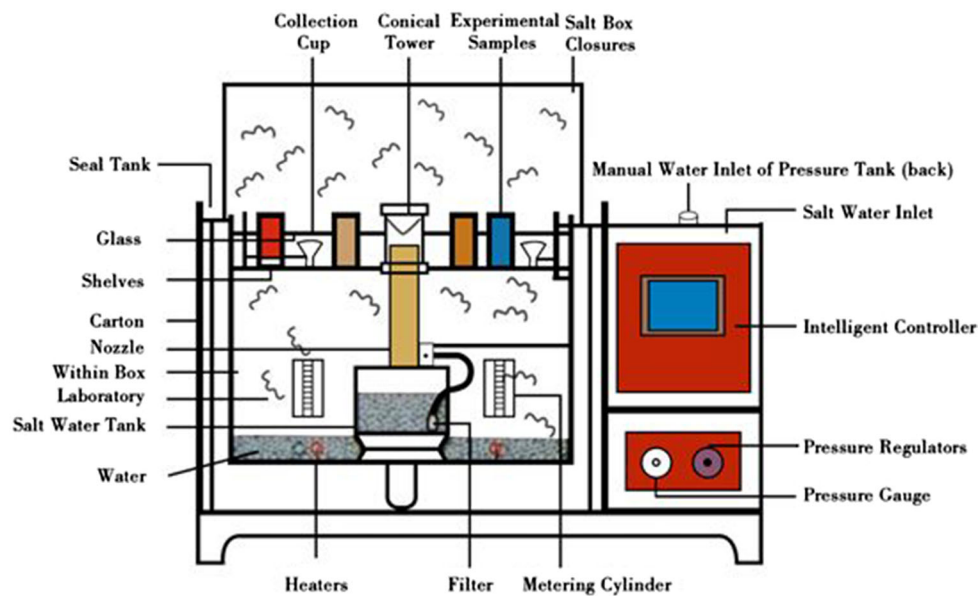


**Fig. 1** Salt-fog corrosion test setup

was refined into ultrafine grains (Ref 25). The weld seam and weld toe surface were treated by the ultrasonic impact method to create a plastic deformation layer up to 300  $\mu\text{m}$ . The ultrasonic impact treatment had a distinct effect on the corrosion resistance of the 16MnR welded joint (Ref 27).

Although significant progress has been made to improve fatigue life of welded joints using UIT, it has not been reported that UIT is used to improve the SCC resistance of welded joints of high-strength aluminum alloys. This paper introduces UIT for controlling the residual stress of welded joints of 6005A aluminum alloy in high-speed trains to improve the SCC resistance of welded joints. The effect of UIT on the residual stress, hardness, strength, and corrosion resistance of welded aluminum joints was investigated. It was found that UIT could harden the surface of the welded area and produce beneficial compressive residual stress, which could improve the SCC resistance of welded joints. Moreover, the evolution of residual stress of welded joints without and with UIT was studied using a salt-fog corrosion test. Experimental results showed that significantly lower stress was observed on the samples with UIT than without UIT after exposure to a corrosive environment for 14 days, greatly reducing the SCC tendency.

## 2. Experimental Procedure

### 2.1 Materials and Welding Process

The chemical compositions of base materials (6005 A) and filler metal (ER5356) are listed in Table 1. The base material 6005 A is 4-mm-thick sheets with T6 heat treatment (treated by solution heat treatment and then artificially aged according to ISO 2107:2007). Table 2 shows the mechanical properties of the base materials and the filler metal. The strength of the filler metal is lower than the base materials of 6005A-T6.

### 2.2 Welding Process

Gas metal arc welding (GMAW) process was used to weld the test samples. The filler wire was ER5356 with a diameter 1.6 mm and the shielding gas was 99.999% pure argon. Before welding, the surface of the base metals was chemically cleaned to remove the oxides in order to decrease the porosity propensity of the weld joints. The welding parameters used to weld 6005A-T6 are shown in Table 3. The dimensions of welded samples were 350-mm long and 210-mm wide.

### 2.3 Salt-Fog Corrosion Test

Salt-fog corrosion is a corrosion process that is mainly controlled by oxygen depolarization reactions and accelerated by  $\text{Cl}^-$  ions. The cathode potential of oxygen ions is 0.805 V and the anode potential of aluminum alloy is  $-0.85$  V (Ref 30). Therefore, a battery is formed between anodal aluminum ions and cathodal oxygen ions. A dense oxide film is formed during the initial corrosion stage. Thus, only a small quantity of  $\text{Cl}^-$  and  $\text{O}^{2-}$  could penetrate the oxide film and then go into the inner structure of the aluminum alloy to form pitting corrosion. As the corrosion time increases, the quantity of  $\text{Cl}^-$  and  $\text{O}^{2-}$  in the inner structure of the aluminum alloy becomes greater, inducing pitting corrosion caves.

A salt-fog test determined the corrosion resistance of materials due to electrochemical reaction and studied the material accelerated stress corrosion. The equipment used was a

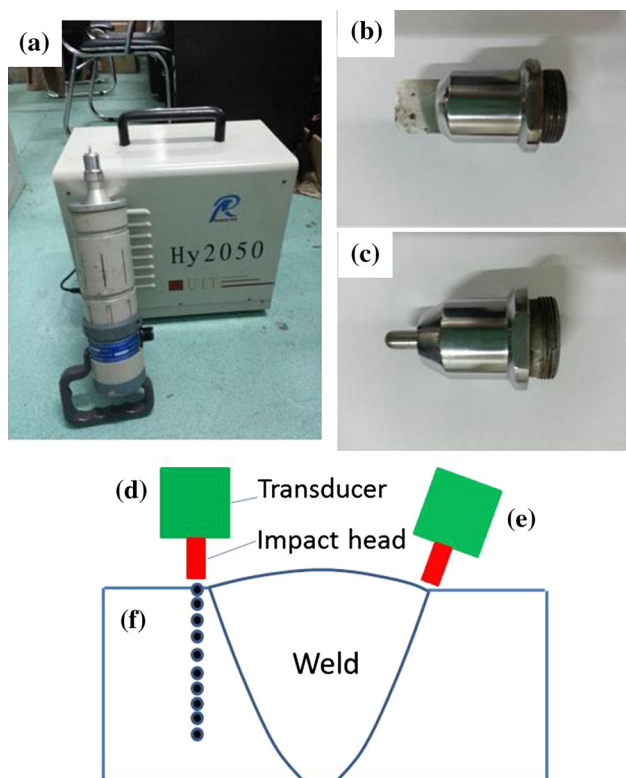


**Fig. 2** Ultrasonic impact treatment of a weldment: (a) UIT equipment; (b) strip head; (c) rod head; (d) UIT position 1; (e) UIT position 2; and (f) a weld cross-section

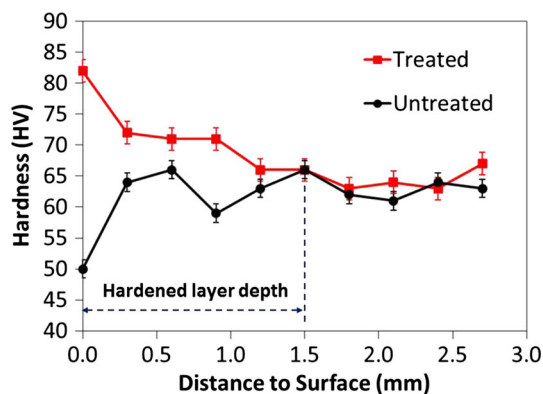


**Fig. 3** Effect of ultrasonic impact treatment on hardness

**Table 4** The selected parameters for ultrasonic impact treatment

Frequency, Hz	Power, W	Maximum amplitude, $\mu\text{m}$	Impact current, A	Impact time, s
19150	1000	50	2.2	90

SO2/Q-0250 salt-spray test chamber, as schematically shown in Fig. 1.

Solid NaCl and deionized water (ph value between 6.5 and 7.2) were mixed in a salt-water tank to form 5% NaCl solution. The solution transformed into salt spray at a pressure of 0.09 MPa in the conical tower. During the experiment, the temperature in the salt-fog cabinet was kept at 35 °C. Samples were polished using sand papers to remove oxides, cleaned by acetone, etched in 10% NaOH solution for 10 minutes, cleaned by water, and immersed into HNO<sub>3</sub> to achieve a shining surface. After cleaning and drying, samples were placed into a salt-fog cabinet with a 30° angle between the test surface and vertical direction.

To check the effect of corrosion time on material corrosion behavior, the salt-fog test was conducted for both the as-weld sample and the treated sample. The experiment was conducted based on the salt-fog corrosion test standard, GB/T10125-1997 and salt-spray test GB/T 16545-1996.

## 2.4 Surface Profile Examination

Surface profiles were examined before and after the salt-fog corrosion test. A JSM-6490LV Scanning Electron Microscope and a VK-9700K color laser scanning microscope were used to observe the surface profile after UIT and after corrosion.

## 2.5 Hardness and Tensile Test

Hardness was measured after UIT with a Vickers Hardness (HV-10B) tester based on metal hardness standard GB/T4340-2009. The load was 98 N and lasted for 10 s.

Tensile strength test was performed on a WDW3100 electronic universal testing machine with a loading speed of 1 mm/min based on the tensile testing method, GBT 2651-2008 and GB/T 228-2010.

## 2.6 Ultrasonic Impact Treatment

Ultrasonic impact treatment is a mechanical treatment method that can be applied to a weld to produce compressive residual stresses and locally modify the weld geometry. The

equipment of ultrasonic impact treatment consists of a power control, an ultrasonic impact gun, and an impact head, as shown in Fig. 2. Ultrasonic impact treatment works by converting harmonic resonations of an acoustically tuned body energized by an ultrasonic transducer into mechanical impulses imparted onto the surface of the material being treated.

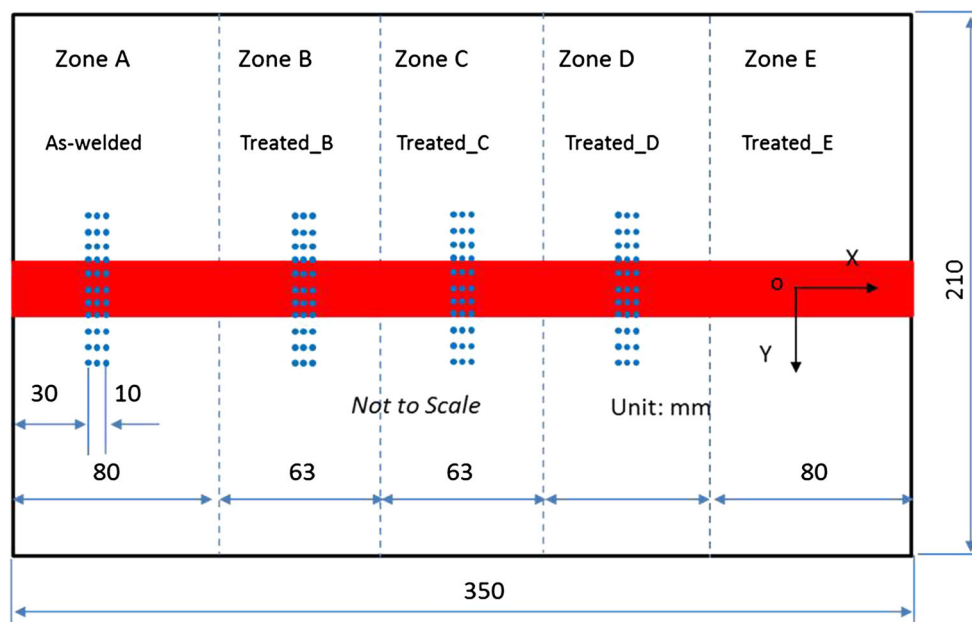
HY2050 UIT equipment has two types of ultrasonic impact head, as shown in Fig. 2(b) and (c). The strip impact head was used to treat the weld and heat-affected zone (HAZ), and the rod impact head was used to treat the weld toe. Under the same parameter setting, the rod impact head can produce more pressure than the strip impact head, resulting in high compressive stress, while the strip impact head can impact more areas than the rod impact head, resulting in a time-efficient treatment. UIT can be mechanically controlled to provide repeatability of results from one application to the next. For many applications, UIT is most effectively employed by hand. The force imparted to the weld in the UIT process is controlled by the operator.

Figure 2(d) and (e) illustrate the UIT applied on a weldment (Fig. 2f). A 90° angle between the impact head and treated area is preferred to achieve an effective treatment, as shown in Fig. 2(d). To treat the weld toes, the impact head has to be rotated to accommodate the shape of weld toes, as shown in Fig. 2(e). The high portability of the UIT system enables it to austere locations and hard-to-reach places. Since mechanically controlled UIT is difficult to implement in the production of high-speed trains, manual operation of UIT was applied in this study.

The parameters of ultrasonic impact treatment including frequency, power, ultrasonic amplitude, impact time, and impact

**Table 5 Effect on UIT on tensile strength of welded joints**

Sample	Tensile strength, MPa	Elongation, %
Before UIT	191.52	5.47
After UIT	215.42	3.52



**Fig. 4** Sample and measured location in the welded specimen

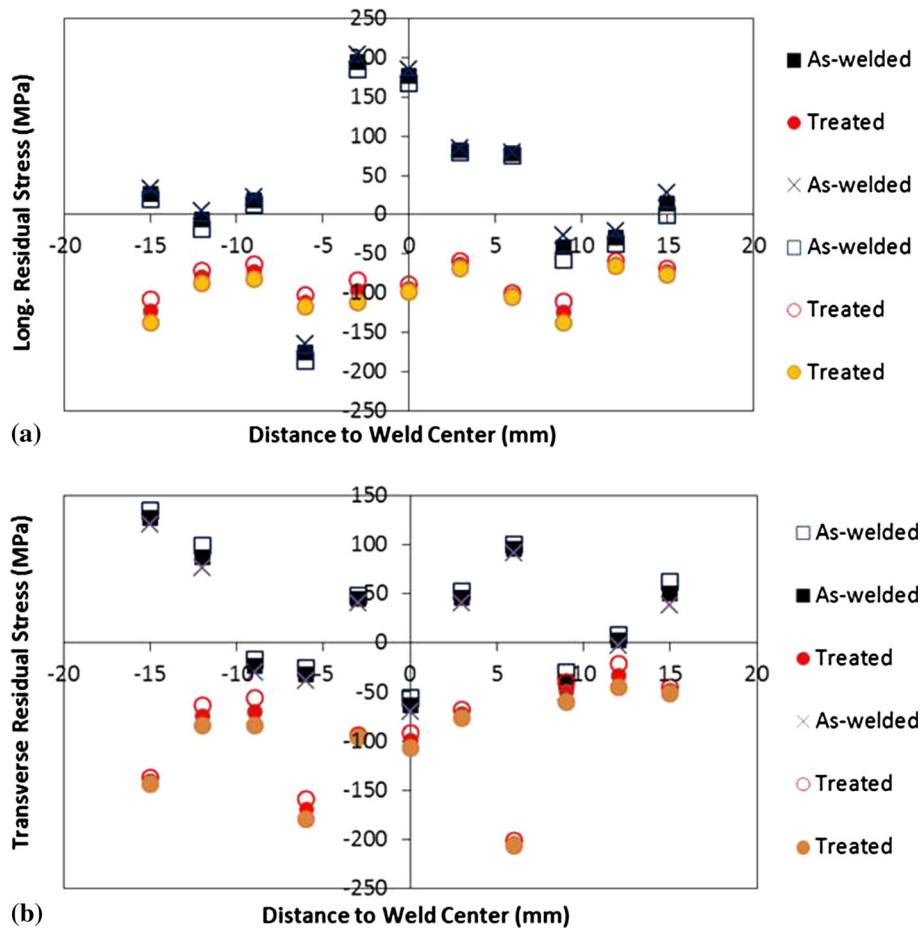


Fig. 5 Effect of UIT on residual stress: (a) longitudinal and (b) transverse

current are shown in Table 4. The parameters were selected based on experience in treating other high-strength aluminum alloys.

### 2.7 Residual Stress Measurement

The residual stresses of welded samples at as-welded conditions and after salt-fog corrosion testing were evaluated using x-ray diffraction residual stress measurement. The measuring equipment was iXRD residual stress evaluation machine. The measurements were conducted based on the EN 15305-2008 non-destructive testing method for residual stress analysis.

In x-ray diffraction residual stress measurement, the strain in the crystal lattice is measured, and the residual stress producing the strain is calculated, assuming a linear elastic distortion of the crystal lattice. Although the term stress measurement has come into common usage, stress is an extrinsic property that is not directly measurable. All methods of stress determination require measurement of some intrinsic property, such as strain, force or area, and the calculation of the associated stress.

## 3. Results and Discussion

### 3.1 Effect of UIT on Hardness

Hardness samples were prepared by cutting the weld joint of an untreated sample and a treated sample in the direction perpendicular to the welding direction. Hardness tests were

conducted in the HAZ of the welded joints. The measured points started from the weld top surface and moved along the thickness direction, as shown in Fig. 2(f).

Figure 3 shows the measured Vickers hardness for the untreated sample and the treated sample through plate thickness. For the untreated sample (as-welded sample), the hardness was lower than the material nominal hardness (100 HV), as shown in Table 2, and slightly increased along the thickness direction. This is because the welding process destroys the original material heat treatment conditions and creates a softening zone in the HAZ of the welded joint, which is a common problem during welding of 2000 and 6000 series of high-strength aluminum alloys. The welding-induced temperature is higher on the weld top surface of the weldment, which results in a lower thickness. After the ultrasonic impact treatment, the hardness significantly increases on the plate surface. The hardness for the treated sample decreased along thickness direction. At 1.5 mm from the plate surface, the same hardness was measured between the treated sample and the untreated sample, which implied the effective treatment thickness is 1.5 mm for the parameters shown in Table 4. Since the hardness is related to the material strength, it is expected that ultrasonic impact treatment can help improve the HAZ softening issue and increase the strength of the welded joint.

### 3.2 Effect of UIT on Residual Stress

To evaluate the effectiveness of the UIT parameters, longitudinal (X direction) and transverse (Y direction) residual

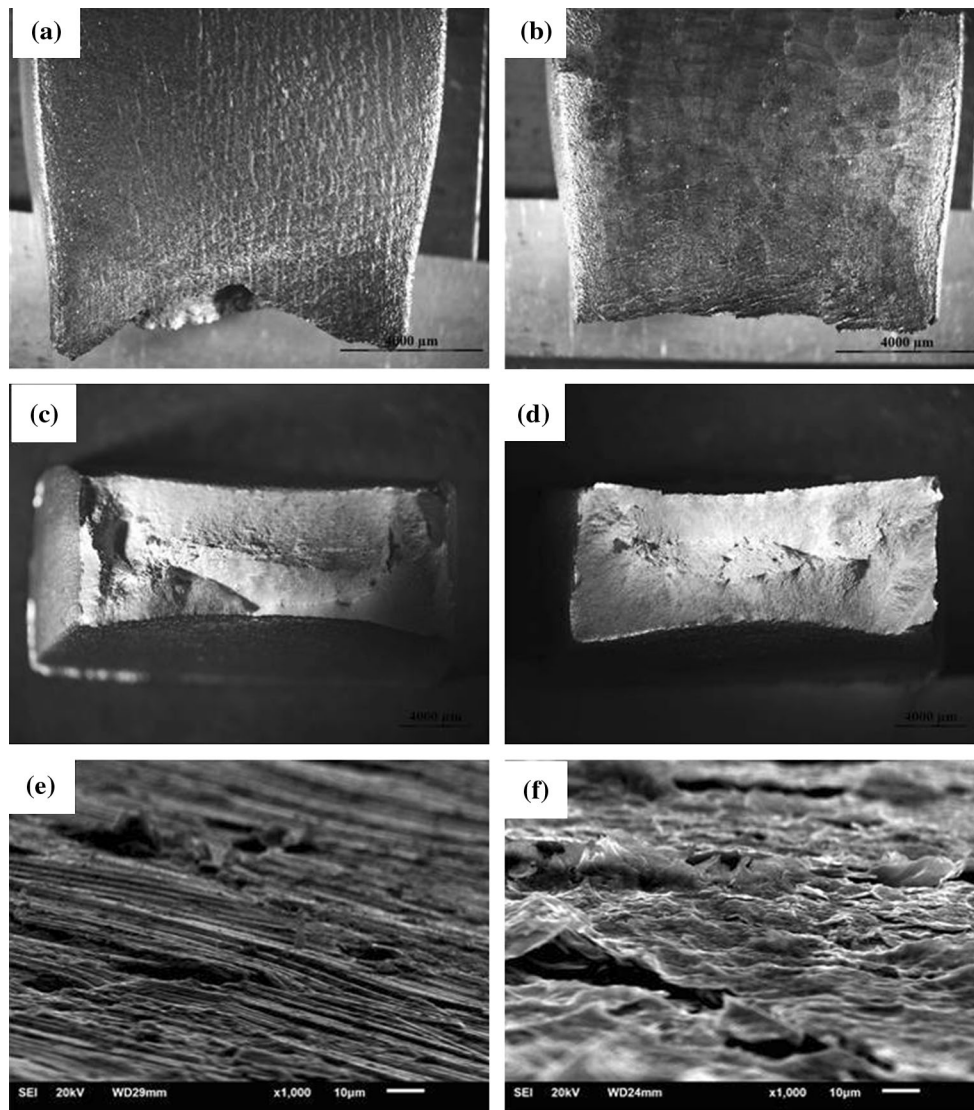


**Fig. 6** Fracture surface of a untreated sample and a treated sample after tensile tests: (a) a broken untreated sample; (b) a broken treated sample; (c) cross-section of untreated sample; (d) cross-section of treated sample; (e) untreated sample fracture surface morphology; and (f) treated sample fracture surface morphology

stresses were measured for both the as-welded sample and the treated samples at points that were located in the weld and HAZ, as shown in each zone of Fig. 4.

Figure 5 shows the measured longitudinal and transverse residual stresses for the as-welded and the treated samples. Both the longitudinal residual stress and transverse residual stress become compressive after ultrasonic impact treatment. Higher compressive residual stresses are observed at the weld toes (about 6 mm away from the weld center), which could result from the rod impact head. The rod impact head produces more pressure during treatment than the strip impact head. Therefore, the impact parameters shown in Table 4 are effective in treating the weld area to induce compressive residual stress.

Both ultrasonic waves and mechanical impacts can contribute to production of compressive residual stress in the weld region (Ref 23, 31, 32). In UIT, an acoustically tuned resonator bar (impact head) is induced to vibrate by energizing it with a magnetostrictive or piezoelectric ultrasonic transducer. The

energy generated from these high frequency impulses is imparted to the treated surface through the contact of specially designed impact heads. The impact head acoustically couples with the work piece, creating harmonic resonance. This harmonic resonance is performed at a carefully calibrated frequency, to which metals respond very favorably, resulting in compressive residual stress, stress relief, and grain structure improvements. The effect of treatment depends on a combination of different frequencies and displacement amplitude.

### 3.3 Effect of UIT on Welded Joint Strength

Welded joint strength was examined by tensile tests before and after UIT. Table 5 shows a comparison of tensile strength and elongation between untreated and treated samples. The tensile strength of the untreated sample is about 191.52 MPa (see Table 5), which is lower than the tensile strength of both the base material (A6005-T6) and the filler metal (ER5356), as

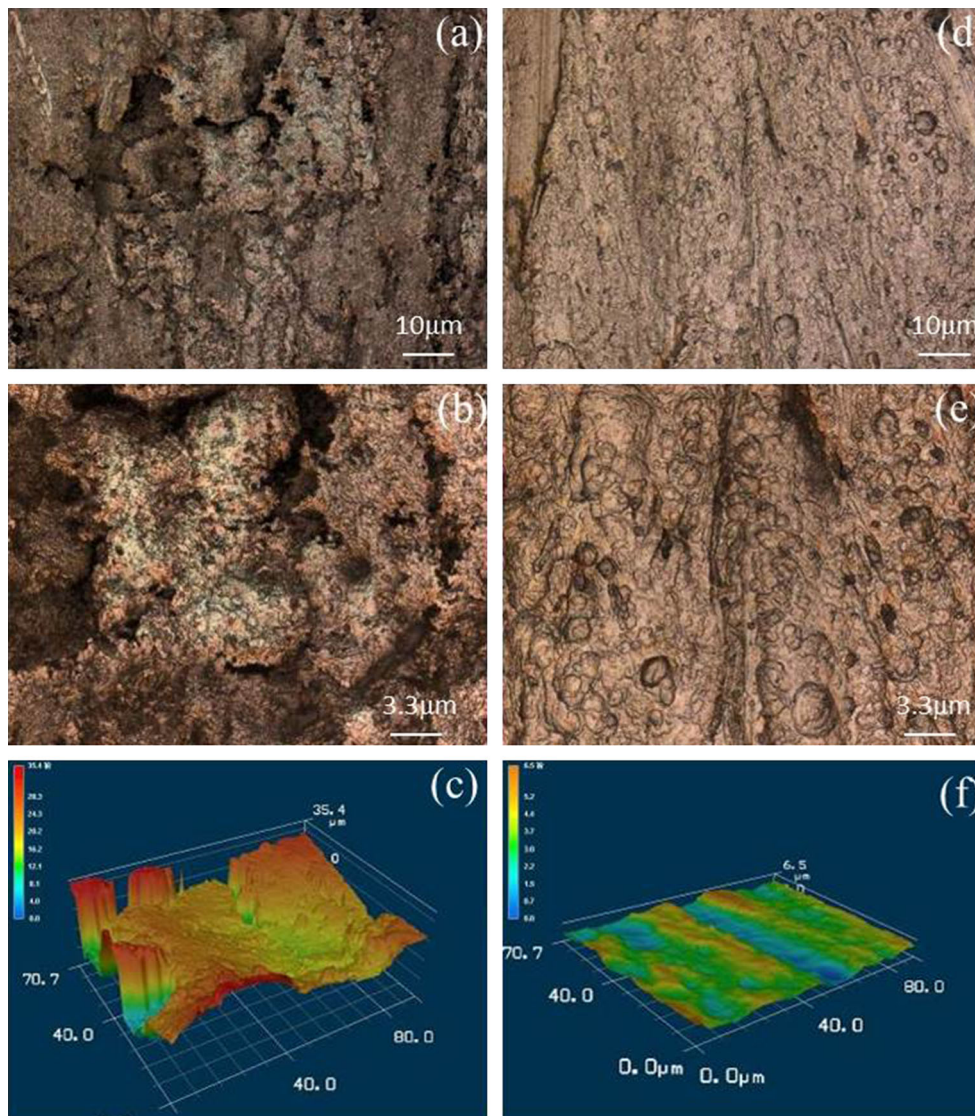


**Fig. 7** Surface profile of weld and HAZ after corrosion for 14 days: (a, b) untreated samples; (c) surface flatness of untreated sample; (d, e) treated samples; and (f) surface flatness of treated sample

shown in Table 2. This is typical when welding heat treatment strengthened aluminum alloys as welding-induced heat damages the heat treatment conditions of these aluminum alloys, resulting in softening of the HAZ.

After UIT, the tensile strength of welded joints is about 215 MPa, which is about 24 MPa higher than the untreated sample. This could result from two factors: work hardening and compressive residual stress on the treated area. Table 5 shows that the treated sample (elongation 3.5%) had a slightly lower elongation than the untreated sample (elongation 5.5%), which confirms the effect of work hardening on UTS. Compressive residual stress could contribute to the UTS increase since the tensile stress induced in the tensile tests needs to overcome the compressive residual stress first and then increases until the failure of samples.

In addition, ultrasonic impact treatment can refine the microstructure in the impact region due to rapid friction heating and cooling combined with severe plastic deformation. Gao et al. studied the effect of ultrasonic impact treatments on the

microstructure of weld toes in a six-pass welded joint. It was found that after the treatment, a very fine microstructure was formed immediately under the weld toe up to 75  $\mu\text{m}$ . The fine microstructure could also result in the increase of welded joint tensile strength.

Figure 6 shows broken samples and fracture surfaces without UIT (untreated) and with UIT (treated) after tensile tests. The untreated sample was more ductile than the treated sample. More plastic deformation was shown on the untreated sample (Fig. 6c) than on the treated sample (Fig. 6d). This is because work hardening is induced on the treated sample by UIT and results in lower elongation of the treated sample, as shown in Table 5. The fine grains and dislocation intersections on the treated sample also increased the difficulty of cracking propagation during tensile testing. The untreated sample showed fibrous microstructure and rolling patterns (Fig. 6e) which resulted from material milling, while the treated sample showed uneven morphology (Fig. 6f), which could result from plastic deformation and the fine microstructure induced by UIT.

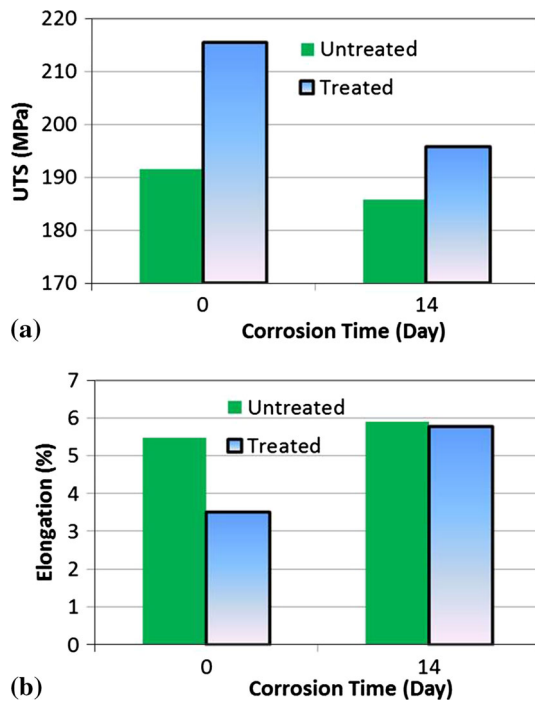


**Fig. 8** Effect of corrosion time on ultimate tensile strength and elongation: (a) UTS and (b) elongation

In addition, pores were found on the untreated sample (Fig. 6e), while pores are distorted and covered on the treated sample (Fig. 6f), which could induce higher strength during tensile testing.

### 3.4 Effect of UIT on Surface Profile of Corrosion Samples

Continuous salt-fog tests were conducted for as-welded samples (untreated) and ultrasonic impact-treated samples. The effect of corrosion on the surface profile was studied on both untreated and treated samples to check the effectiveness of UIT to improve corrosion resistance of the welded joints of 6005A-T6 aluminum alloy.

Surface profiles on both the untreated and treated samples were examined in the weld and HAZ using a laser scanning digital microscope. Corrosion pits and corrosion-produced products were observed on the surface of the untreated sample after corrosion for 14 days, as shown in Fig. 7(a) ( $\times 1000$  magnification) and Fig. 7(b) ( $\times 3000$  magnification). The laser scanned surface plot (Fig. 7c) showed the corrosion pits propagated into the thickness. The deepest pit was about  $35.4\text{-}\mu\text{m}$  deep and the area of corrosion pits was about 43.6% of the scanned area. Considerably less corrosion pits were observed on the surface of the treated sample than the untreated sample, as shown in Fig. 7(d) ( $\times 1000$  magnification) and Fig. 7(e) ( $\times 3000$  magnification). The laser scanned surface profile (Fig. 7f) showed the deepest pit on the treated sample was  $6.5\text{ }\mu\text{m}$  deep. The area of corrosion pits was about 27.7% of the scanned area. Both the depth and the area of corrosion pits on the treated sample were much smaller than that on the untreated sample. Therefore, the treated sample has much better resistance of corrosion than the untreated sample.

### 3.5 Effect of UIT on Welded Joint Strength of Corrosion Samples

Welded joint strength was examined by tensile tests before the corrosion test (0 day) and after the corrosion test to investigate the effect of the corrosion time on ultimate tensile strength (UTS) and elongation of welded joints for the untreated samples and the treated samples. As shown in Fig. 8(a), the ultimate tensile strengths of both the untreated samples and the treated samples decrease after corrosion for 14 days. For the untreated sample, the elongation of the untreated sample did not have a significant change after corrosion for 14 days (Fig. 8b). The UTS reduction could be due to the corrosion pits shown in Fig. 7(a). Cracks could have initiated on the corrosion pits due to the stress concentration during tensile tests. For the treated sample, UTS has a 9% reduction after corrosion for 14 days, while elongation was similar to the untreated sample after corrosion for 14 days. The extent of the work hardening effect resulting from the UIT may reduce because of the corrosion, which results in a similar elongation between the treated sample and untreated sample after corrosion for 14 days.

### 3.6 Effect of UIT on Residual Stress Distributions on Corrosion Samples

Figure 9 shows the effect of corrosion on the longitudinal residual stress for the untreated samples (Fig. 9a) and for the treated samples (Fig. 9b). After 14-day corrosion, the treated sample had much lower longitudinal tensile stress than the untreated sample.

For the untreated samples that did not go through corrosion test (0 day in Fig. 9a), high tensile stress was shown in the middle of the weld, which is balanced by low compressive stress at each side of the weld. This distribution is a nominal longitudinal residual stress distribution for a single-pass butt joint. After 14-day corrosion, the longitudinal residual stress on the untreated sample was re-distributed, but the maximum stress value did not have a significant change, as shown in Fig. 9(a).

For the treated samples without going through corrosion test (0 day in Fig. 9b), high compressive longitudinal is shown in the welded joints. After 14-day corrosion, the compressive longitudinal residual stress magnitudes were reduced, but stresses at most points were in compressive, as shown in Fig. 9(b).

Figure 10 shows the effect of the corrosion on transverse residual stress for the untreated sample (Fig. 10a) and the treated sample (Fig. 10b). After 14-day corrosion, the treated sample had a much lower transverse tensile stress than the untreated sample. For the untreated sample, transverse tensile stress magnitude in the weld increased after corrosion, as shown in Fig. 10(a). For the treated sample, transverse stress magnitude also increased and the transverse residual stresses at the weld toes are in tension after corrosion, as shown in Fig. 10(b).

Corrosion tests showed that the compression resulted from UIT was reduced after 14-day corrosion. This could be due to corrosion media diffusing into the materials under the treated area. The diffused corrosion media would alter the material crystal lattice so that to affect the plastic deformation zone and relief the UIT-induced compressive residual stress. The exact mechanism how corrosion affect the residual stress needs further study, which will be discussed in a future publication.

The residual stress measurements suggest that the treated sample has much lower tensile residual stress than the untreated

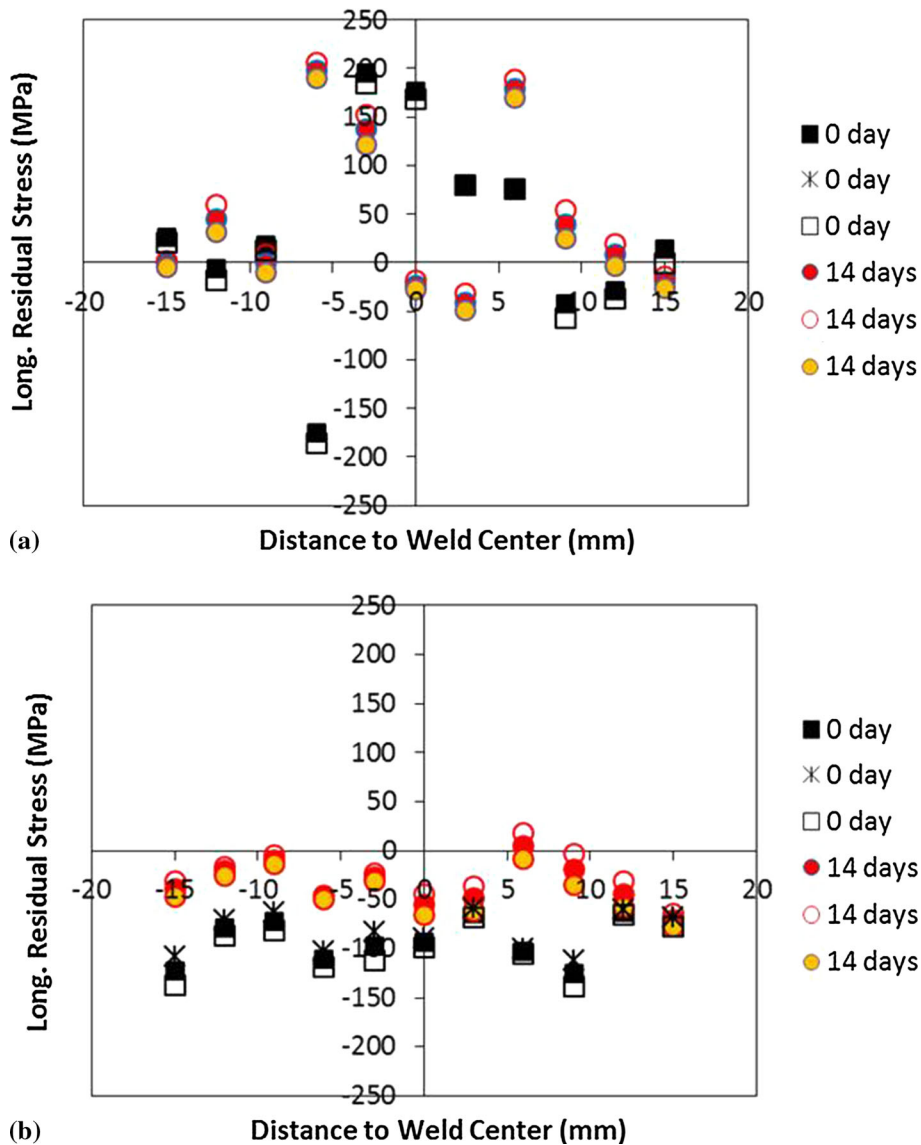


**Fig. 9** Effect of corrosion on longitudinal residual stress: (a) untreated sample and (b) treated sample

samples during corrosion. Although low tensile longitudinal and transverse residual stresses appear at the weld toes after the 14-day corrosion, the welded joints in the high-speed trains could still be safe during service since the corrosion environment in the salt-fog test is far more corrosive than in the service environment of high-speed trains. Therefore, ultrasonic impact treatment is an effective technique to control the stress state of aluminum-welded joints for corrosion environment to improve the SCC resistance.

#### 4. Conclusion

GMAW process was used to weld specimens made of 6005A-T6 aluminum alloy that was selected as the main materials for the components of high-speed trains. Ultrasonic impact treatment was applied on the weld region to improve the stress corrosion cracking resistance. Salt-fog corrosion tests were conducted for the as-welded joints and the ultrasonic

impact-treated weld joints to study the tensile strength and stress changes during corrosion. Based on the testing results, the following conclusions could be drawn:

- Ultrasonic impact treatment process was effective in producing compressive longitudinal and transverse residual stress in the welded joints. The effective depth of ultrasonic impact treatment depth was 1.5 mm.
- The effective parameters of ultrasonic impact treatment for the welded joints of 6005A-T6 aluminum alloy were a frequency of 19.15 kHz, a power of 1 kW, a maximum amplitude of 50  $\mu\text{m}$ , an impact time of 2.2 A, and an impact time of 90 s.
- Ultrasonic impact treatment resulted in the increases of hardness and tensile strength of welded joints. The treated sample had higher strength and lower tensile residual stress than the untreated sample during corrosion.
- Ultrasonic impact treatment was an effective technique to improve the stress corrosion cracking resistance of the welded joints of 6005A-T6 aluminum alloy.

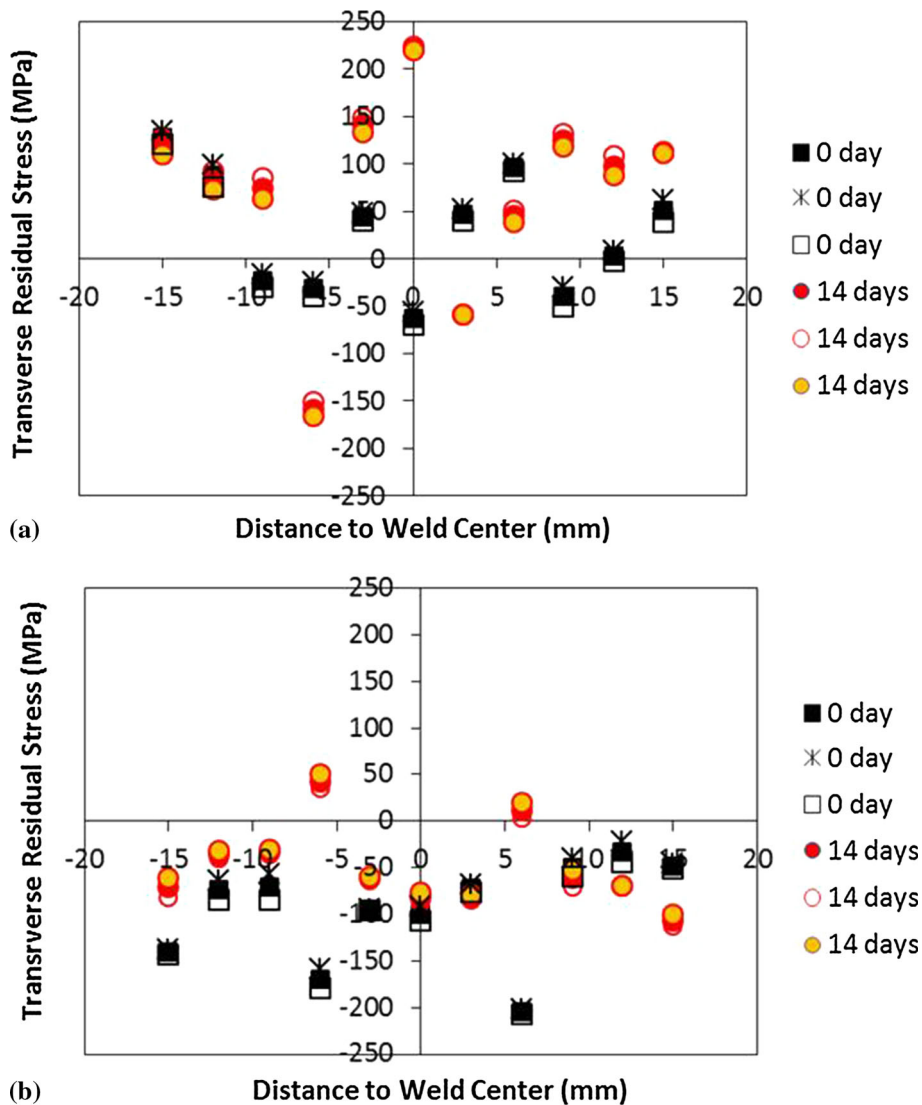


Fig. 10 Effect of corrosion on transverse residual stress: (a) untreated sample and (b) treated sample

### Acknowledgment

The results of this paper were from the project, “effect of residual stress on the corrosion behavior in weld joints and Development of control technology for car bodies in aluminum-alloy trains” and the Pillar Projects in the National Science and Technology. The authors acknowledge the financial support by the scientific and technological innovation projects of Chinese Central universities (No. 2682014CX003) and the financial support by the National Science & Technology Pillar Program (No. 2015BAG12B01).

### References

1. Y. Deng, R. Ye, G. Xu, J. Yang, Q. Pan, B. Peng, X. Cao, Y. Duan, Y. Wang, L. Lu, and Z. Yin, Corrosion Behaviour and Mechanism of New Aerospace Al-Zn-Mg Alloy Friction Stir Welded Joints and the Effects Of Secondary Al<sub>3</sub>ScxZr<sub>1-x</sub> Nanoparticles, *Corros. Sci.*, 2015, **90**, p 359–374
2. J. Liu, X. Hao, S. Li, and M. Yu, Stress Corrosion Cracking Model Based on Experiment and Gray Theory For High Strength Aluminum Alloy, *J. Mater. Eng.*, 2011, **1**(3), p 60–64
3. K.C. Jang, D.G. Lee, J.M. Kuk, and I.S. Kim, Welding and Environmental Test Condition Effect in Weldability and Strength of Al Alloy, *J. Mater. Process. Technol.*, 2005, **164–165**, p 1038–1045
4. C.S. Paglia and R.G. Buchheit, A Look in the Corrosion of Aluminum Alloy Friction Stir Welds, *Scr. Mater.*, 2008, **58**, p 383–387
5. D.A. Wadson, X. Zhou, G.E. Thompson, P. Skeldon, L.D. Oosterkamp, and G. Scamans, Corrosion Behavior of Friction Stir Welded AA7108- T79 Aluminum Alloy, *Corros. Sci.*, 2006, **48**, p 887–897
6. Z.Y. Wang, T. Ma, W. Han, and G.C. Yu, Corrosion Behavior on Aluminum Alloy LY12 In Simulated Atmospheric Corrosion Process, *Trans. Nonferr. Met. Sci. China*, 2007, **17**(2), p 326–334
7. X. Zhang, C. Ma, G. Gou, Y. Liu, H. Chen, and H. Li, Failure Analysis of A7N01S-T5 Aluminum Alloy Crossbeam for High Speed Train, *Corros. Prot.*, 2013, **34**(3), p 258–261
8. R. Zhu, W. Dong, H. Lin, S. Lu, and D. Li, Finite Element Simulation of Welding Residual Stress for Buffer Beam of CRH2A High Speed Train, *Acta Metall.*, 2014, **50**(8), p 944–954
9. G. Gou, N. Huang, H. Chen, H. Liu, A. Tian, and Z. Guo, Research on Corrosion Behavior of A6N01S-T5 Aluminum Alloy Welded Joint for High-Speed Trains, *J. Mech. Sci. Technol.*, 2012, **26**(5), p 1–6
10. The European Union, Design of Aluminum Structures (Part 1-3): Structures Susceptible to Fatigue, The European Union per Regulation 305/2011, Directive98/34/EC, Directive 2004/18/EC
11. H.E. Coules, Contemporary Approaches to Reducing Weld Induced Residual Stress, *Mater. Sci. Technol.*, 2013, **29**(1), p 4–18

12. Y.P. Yang and G. Jung, Advancement in Prediction and Control of Welding Residual Stress and Distortion, *Mater. Sci. Forum*, 2007, **539–543**, p 3943–3948
13. Z.Y. Zhu, C.Y. Deng, Y. Wang, Z.W. Yang, J.K. Ding, and D.P. Wang, Effect of Post Weld Heat Treatment on the Microstructure and Corrosion Behavior of AA2219 Aluminum Alloy Joints Welded by Variable Polarity Tungsten Inert Gas Welding, *Mater. Des.*, 2015, **65**, p 1075–1082
14. Y.P. Yang, Understanding of Vibration Stress Relief with Computation Modeling, *J. Mater. Eng. Perform.*, 2008, **18**(7), p 856–862
15. Y.P. Yang and P. Dong, Buckling Distortions and Mitigation Techniques for Thin-Section Structures, *J. Mater. Eng. Perform.*, 2012, **21**(2), p 153–160
16. J.T. Wang, Y.K. Zhang, J.F. Chen, J.Y. Zhou, M.Z. Ge, Y.L. Lu, and X.L. Li, Effects of Laser Shock Peening on Stress Corrosion Behavior of 7075 Aluminum Alloy Laser Welded Joints, *Mater. Sci. Eng., A*, 2015, **647**, p 7–14
17. S. Sathyajith and S. Kalainathan, Effect of Laser Shot Peening on Precipitation Hardened Aluminum Alloy 6061-T6 Using Low Energy Laser, *Opt. Lasers Eng.*, 2012, **50**(3), p 345–348
18. K. Li, X. Fu, R. Li, P. Gai, Z. Li, W. Zhou, and G. Chen, Fretting Fatigue Characteristic of Ti-6Al-4V Strengthened by Wet Peening, *Int. J. Fatigue*, 2016, **85**, p 65–69
19. S. Roy, J.W. Fisher, and B.T. Yen, Fatigue Resistance of Welded Details Enhanced by Ultrasonic Impact Treatment (UIT), *Int. J. Fatigue*, 2003, **25**(9–11), p 1239–1247
20. V.M. Nadutov and D.V. Semenov, Mossbauer Effect in f.c.c. Fe–Ni–C Alloys after the Ultrasonic Impact Surface Treatment, *J. Phys.*, 2005, **55**(1), p 835–843
21. I. Weich and T. Ummenhofer, Effects of High-Frequency Peening Methods on the Surface Layers and the Fatigue Strength of Welded Details, *Mater. Manuf. Processes*, 2011, **26**(2), p 288–293
22. G.R. Jinu and P. Sathiya, Investigation of the Fatigue Behavior of Butt-Welded Joints Treated by Ultrasonic Peening Process and Compared with Fatigue Life Assessment Standards, *Int. J. Adv. Manuf. Technol.*, 2009, **40**(3), p 74–83
23. H. Gao, R.K. Dutta, R.M. Huizenga, M. Amirthalingam, M.J.M. Hermans, T. Buslaps, and I.M. Richardson, Stress Relaxation due to Ultrasonic Impact Treatment on Multi-Pass Welds, *Sci. Technol. Weld. Joining*, 2014, **19**(6), p 505–513
24. X. An and C.A. Rodopoulos, Study of the Surface Nano-Crystallization Induced by the Ultrasonic Impact Treatment on the Near-Surface of 2024-T351 Aluminum Alloy, *J. Mater. Eng. Perform.*, 2006, **15**(2), p 355–364
25. D. Ahn, k. Shin, J. Dong, J. Jung, and D. Kim, in *Effect of Ultrasonic Shot Peening on the Microstructural Evolution and Mechanical Properties of SUS304*, ed. by Y. Zhang, C.W. Su, H. Xia, P. Xiao. Advanced Materials and Processing (World scientific Publishing Co. Pte. Ltd., 2011), p 83–86
26. X. Ling and G. Ma, Effect of Ultrasonic Impact Treatment on the Stress Corrosion Cracking of 304 Stainless Steel Welded Joints, *J. Press. Vessel Technol.*, 2009, **131**(5), p 051502. doi:10.1115/1.3147988
27. B.L. He, Y.X. Yu, J. Liu, and J.P. Shi, Effect of Ultrasonic Impact Treatment on Corrosion Resistance of Welded Joints of 16MnR Steel, *Adv. Mater. Res.*, 2013, **815**, p 689–694
28. Z. Dong, Z. Liu, M. Li, J. Luo, W. Chen, W. Zheng, and D. Guzonas, Effect of Ultrasonic Impact Peening on the Corrosion Of Ferritic-Martensitic Steels In Supercritical Water, *J. Nucl. Mater.*, 2015, **457**, p 266–272
29. Z. Zhu, Y. Li, X. Wang, and H. Chen, Surface Treatment To Reduce and Redistribute Residual-Stresses in A7N01 Weld By Micro-Arc Oxidation, *J. Mater. Process. Technol.*, 2016, **231**, p 248–253
30. J.R. Davis, Corrosion of Aluminum and Aluminum Alloy, *Corros. Sci.*, 1999, **65**(2), p 1898–1904
31. E.S. Statnikov, Physics and Mechanism of Ultrasonic Impact Treatment, IIR Document XIII-2004-04, 2004
32. Y. Kudryavtsev and J. Kleiman, Fatigue Life Improvement of Welded Elements by Ultrasonic Peening, IIR Document XIII-2010-04, 2004